

Synthesis and Reactivity of 10- and 12-Vertex Cobalt–Monocarborane Anions Containing Multiple Metal Centers

Xiu Lian Lu, Thomas D. McGrath, and F. Gordon A. Stone*

Department of Chemistry & Biochemistry, Baylor University, Waco, Texas 76798-7348

Received February 7, 2006

Treatment of [*closo*-1-CB₇H₈][−] with [Co₂(CO)₈] in THF at room temperature affords the 10-vertex dicobalt–monocarbollide anion [6,10-(μ-CO)-6,6,10,10-(CO)₄-*closo*-6,10,1-CO₂CB₇H₈][−], isolated as the [N(PPh₃)₂]⁺ salt (**6**). The analogous 12-vertex species [N(PPh₃)₂][2,3-(μ-CO)-2,2,3,3-(CO)₄-*closo*-2,3,1-CO₂CB₉H₁₀] (**7**) is obtained similarly from [*arachno*-6-CB₉H₁₄][−] and [Co₂(CO)₈] heated to 50 °C. Both **6** and **7** contain a cobalt–cobalt bond that is bridged by one CO ligand. In contrast, the same cobalt reagent with [*closo*-4-CB₈H₉][−] at room temperature gives the tricobalt species [6,7,10-{Co₂(μ-CO)(CO)₅}-7-(μ-H)-6,6-(CO)₂-*closo*-6,1-CO₂CB₈H₇][−], similarly isolated as its [N(PPh₃)₂]⁺ salt (**8a**). The latter contains a V-shaped tricobalt unit, part of a {Co₃B} butterfly that is edge-fused to a {CoCB₈} cluster. Compounds **6** and **7** with CF₃SO₃Me in CH₂Cl₂–THF (1:1) give the zwitterionic, B-substituted complexes [6,10-(μ-CO)-6,6,10,10-(CO)₄-8-{O(CH₂)₄}-*closo*-6,10,1-CO₂CB₇H₇] (**9**) and [2,3-(μ-CO)-2,2,3,3-(CO)₄-12-{O(CH₂)₄}-*closo*-2,3,1-CO₂CB₉H₉] (**10**), respectively, the latter of which reacts further with PPh₃, undergoing THF ring opening to give [2,3-(μ-CO)-2,2,3,3-(CO)₄-12-{O(CH₂)₄PPh₃}-*closo*-2,3,1-CO₂-CB₉H₉] (**11**). In addition, compounds **6** and **8** react with [CuCl(PPh₃)₄] in the presence of Ti[PF₆], affording trimetallic [7,8,10-{Cu(PPh₃)}-7,8-(μ-H)-2,6,10-(μ-CO)-6,6,10,10-(CO)₄-*closo*-6,10,1-CO₂CB₇H₆] (**12**) and tetrametallic [6,7,8,9,10-{Co₂Cu(μ-CO)(CO)₃(PPh₃)₂}-6-(μ-CO)-7,8,9-(μ-H)₃-6,6-(CO)₂-*closo*-6,1-CO₂CB₈H₅] (**13**), respectively. The novel features in the structures of compounds **6–10** and **13** have been confirmed by X-ray diffraction experiments.

Introduction

The chemistry of smaller monocarborane cages has, of late, seen a resurgence that was initiated by the discovery of the “Brellochs reaction”.¹ This allows access to 10-vertex monocarboranes easily in good yields from commercially available decaborane, which in turn has opened the door for routes to useful quantities of a range of 7–10-vertex monocarboranes.^{2–5} Taking advantage of this, we are extending our studies on metal–monocarbollide chemistry, which formerly were restricted to MCB₁₀ species,^{6,7} to encompass clusters with 11 vertexes and fewer. This latter area had previously received only scant attention,⁸ as a consequence of the hitherto poor avail-

ability of small monocarborane precursors.⁹ To this end we initially prepared 11-vertex {*closo*-1,2-MCB₉} metal–monocarbollide complexes containing rhenium,¹⁰ manganese,¹¹ and molybdenum¹² centers.

More recently, we have also focused on reactions of these smaller monocarboranes with iron carbonyls. Thus, the 8-vertex carborane [*closo*-1-CB₇H₈][−] reacts with [Fe₃(CO)₁₂] to successively insert {Fe(CO)₃} moieties, giving the 9- and 10-vertex anions [7,7,7-(CO)₃-*closo*-7,1-FeCB₇H₈][−] (**1**) and then [6,6,6-10,10,10-(CO)₆-*closo*-6,10,1-Fe₂CB₇H₈][−] (**2**), respectively (see Chart 1).¹³ The same iron reagent similarly reacts with 9-vertex [*closo*-4-CB₈H₉][−] to afford 10-vertex [6,6,6-(CO)₃-*closo*-6,1-FeCB₈H₉][−] (**3**).¹⁴ In contrast, the 9-vertex open-cage species [*arachno*-4-CB₈H₁₄][−] with [Fe₃(CO)₁₂] gives the unusual diiron species [4,9-{Fe(CO)₄}-9,9,9-(CO)₃-*arachno*-9,6-FeCB₈H₁₁][−] (**4**), which, upon thermolysis, gives [2,2,2-(CO)₃-*closo*-2,1-FeCB₈H₉][−] (**5**), an isomer of **3**.¹⁴ These findings prompted us to investigate the reactivity of other transition-metal carbonyl reagents with these and related smaller monocarborane cages. We herein report the results of the reactions of {CB₇}, {CB₈},

* To whom correspondence should be addressed. E-mail: gordon_stone@baylor.edu.

(1) Brellochs, B. In *Contemporary Boron Chemistry*; Davidson, M. G., Hughes, A. K., Marder, T. B., Wade, K., Eds.; Royal Society of Chemistry: Cambridge, U.K., 2000; p 212.

(2) Stibr, B. *Pure Appl. Chem.* **2003**, *75*, 1295.

(3) Stibr, B.; Tok, O. L.; Milius, W.; Bakardjiev, M.; Holub, J.; Hnyk, D.; Wrackmeyer, B. *Angew. Chem., Int. Ed.* **2002**, *41*, 2126.

(4) (a) Franken, A.; Kilner, C. A.; Thornton-Pett, M.; Kennedy, J. D. *Collect. Czech. Chem. Commun.* **2002**, *67*, 869. (b) Jelínek, T.; Thornton-Pett, M.; Kennedy, J. D. *Collect. Czech. Chem. Commun.* **2002**, *67*, 1035.

(5) Brellochs, B.; Backovsky, J.; Stibr, B.; Jelínek, T.; Holub, J.; Bakardjiev, M.; Hnyk, D.; Hofmann, M.; Cisarová, I.; Wrackmeyer, B. *Eur. J. Inorg. Chem.* **2004**, 3605.

(6) McGrath, T. D.; Stone, F. G. A. *J. Organomet. Chem.* **2004**, *689*, 3891.

(7) McGrath, T. D.; Stone, F. G. A. *Adv. Organomet. Chem.* **2005**, *53*, 1.

(8) Grimes, R. N. In *Comprehensive Organometallic Chemistry*; Wilkinson, G., Abel, E. W., Stone, F. G. A., Eds.; Pergamon Press: Oxford, U.K., 1982; Vol. 1, Section 5.5. Grimes, R. N. In *Comprehensive Organometallic Chemistry II*; Abel, E. W., Stone, F. G. A., Wilkinson, G., Eds.; Pergamon Press: Oxford, U.K., 1995; Vol. 1, Chapter 9. Grimes, R. N. *Coord. Chem. Rev.* **2000**, *200–202*, 773.

(9) Stibr, B. *Chem. Rev.* **1992**, *92*, 225.

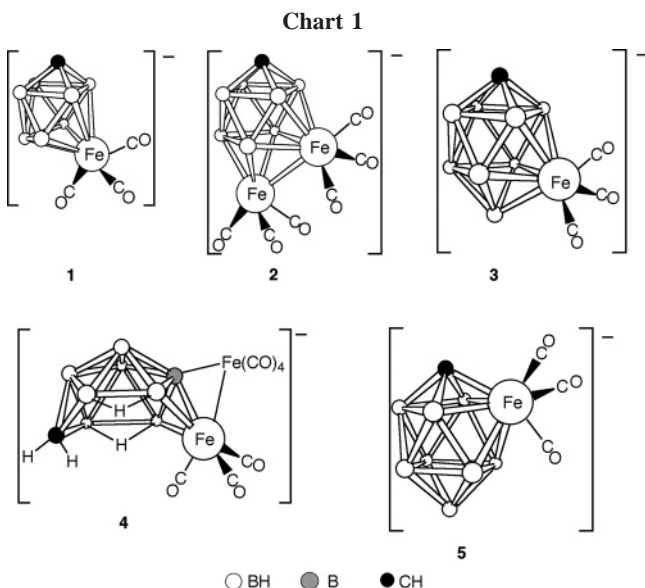
(10) Du, S.; Kautz, J. A.; McGrath, T. D.; Stone, F. G. A. *Organometallics* **2003**, *22*, 2842.

(11) (a) Du, S.; Farley, R. D.; Harvey, J. N.; Jeffery, J. C.; Kautz, J. A.; Maher, J. P.; McGrath, T. D.; Murphy, D. M.; Riis-Johannessen, T.; Stone, F. G. A. *Chem. Commun.* **2003**, 1846. (b) Du, S.; Jeffery, J. C.; Kautz, J. A.; Lu, X. L.; McGrath, T. D.; Miller, T. A.; Riis-Johannessen, T.; Stone, F. G. A. *Inorg. Chem.* **2005**, *44*, 2815.

(12) (a) Lei, P.; McGrath, T. D.; Stone, F. G. A. *Chem. Commun.* **2005**, 3706. (b) Lei, P.; McGrath, T. D.; Stone, F. G. A. *Organometallics*, in press.

(13) Franken, A.; McGrath, T. D.; Stone, F. G. A. *Organometallics* **2005**, *24*, 5157.

(14) Franken, A.; McGrath, T. D.; Stone, F. G. A. *Inorg. Chem.* **2006**, *45*, 2669.

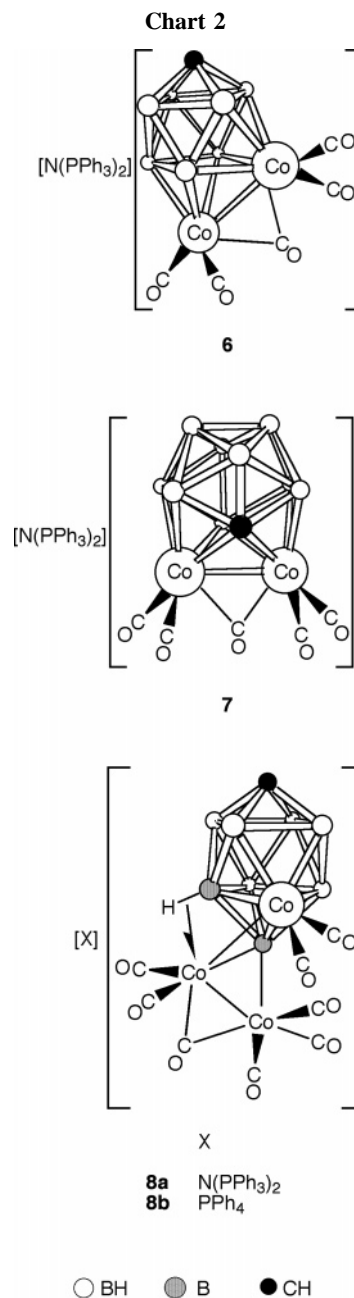


and $\{CB_9\}$ carboranes with the dicobalt reagent $[Co_2(CO)_8]$, along with some preliminary studies of their reactivity toward electrophiles. The species obtained range from 10- to 12-vertex clusters and contain 2, 3, or 4 metal centers.

Results and Discussion

The 10-vertex dicobalt complex $[6,10-(\mu-CO)-6,6,10,10-(CO)_4-closo-6,10,1-CO_2CB_7H_8]^-$ was readily obtained by the reaction of $[NBu^n_4][closo-1-CB_7H_8]$ with $[Co_2(CO)_8]$ in THF (tetrahydrofuran) at room temperature for 5 h. Metathesis to the corresponding $[N(PPh_3)_2]^+$ salt (**6**) (see Chart 2) was easily achieved by addition of $[N(PPh_3)_2]Cl$. In parallel, the analogous 12-vertex cluster $[2,3-(\mu-CO)-2,2,3,3-(CO)_4-closo-2,3,1-CO_2-CB_9H_{10}]^-$ was obtained by the reaction of $[NEt_4][arachno-6-CB_9H_{14}]$ with $[Co_2(CO)_8]$ in THF heated to 50 °C and was similarly isolated as the $[N(PPh_3)_2]^+$ salt (**7**). The anion of **7** was also isolated by treatment of $[NEt_4][nido-6-CB_9H_{12}]$ with $[Co_2(CO)_8]$ in THF at room temperature for 12 h or from the same carborane with $[Co(CO)_3(NO)]$ heated in THF at 40 °C for 16 h.

Compounds **6** and **7** were characterized by the data given in Tables 1 and 2. However, the nature of the anions was initially established by X-ray diffraction studies, the results of which are presented in Figures 1 and 2, respectively. The anions of **6** and **7** consist of closed 10- and 12-vertex dicobaltcarboranes, respectively, with the $\{6,10,1-CO_2CB_7\}$ vertex arrangement in **6** being similar to that in the anion **2**. In both **6** and **7**, the two cobalt centers are mutually adjacent ($Co(6)-Co(10) = 2.4331(3)$ Å in **6**; $Co(2)-Co(3) = 2.4396(2)$ Å in **7**) and the $Co\cdots Co$ vector is bridged by a carbonyl ligand; each of the cobalt vertices also bears two terminal CO groups. This $\{cage\}\cdots\{Co_2(CO)_5\}$ arrangement resembles that of the dicobaltcarborane species $[1,2-(\mu-CO)-1,1,2,2-(CO)_4-4,n-(SR_2)_2-closo-1,2-CO_2B_{10}H_8]$ ($R = Et, n = 7, 11$;¹⁵ $R = Me, n = 11$),¹⁶ which were prepared by reaction of $[Co_2(CO)_8]$ with $[6,9-(SR_2)-arachno-B_{10}H_{12}]$. The $Co\cdots Co$ distances in the three latter dicobalt clusters are 2.488(2), 2.490(1), and 2.4913(4) Å, respectively, somewhat longer than in **6** and **7**. All five of these



$Co\cdots Co$ separations, however, are significantly shorter than in $[Co_2(CO)_8]$.¹⁷

In their IR spectra, both **6** and **7** show several terminal CO stretching bands around $\nu_{max} \sim 1975-2070$ cm^{-1} , plus a medium-intensity band (ν_{max} 1828 (**6**), 1841 cm^{-1} (**7**)) due to the bridging carbonyl. The latter ligand is also evident in the $^{13}C\{^1H\}$ NMR spectrum of **7**, with a characteristic broad signal at δ 258.3, plus two broad peaks at δ 201.2 and 195.4 for two types of terminal CO moieties. This may be interpreted as these groups being static on the NMR time scale, giving a structure in solution that is in agreement with that in the solid state. In comparison, the carbonyl ligands in **6** appear only as two resonances, of which one is broad and the other is very broad (δ 201.1 and 219.9, respectively), with no resonance observed around δ 250 that would be typical for a bridging CO. This is suggestive of some CO exchange between bridging and terminal sites, but with the ligands apparently tending to remain

(15) Schubert, D. M.; Knobler, C. B.; Wegner, P. A.; Hawthorne, M. F. *J. Am. Chem. Soc.* **1988**, *110*, 5219.

(16) Londesborough, M. G. S.; Bould, J.; Holub, J.; Kennedy, J. D.; Thornton-Pett, M.; Stibr, B. *Acta Crystallogr.* **2000**, *C56*, 1423.

(17) Sumner, G. G.; Klug, H. P.; Alexander, L. E. *Acta Crystallogr.* **1964**, *17*, 732. Leung, P. C.; Coppens, P. *Acta Crystallogr.* **1983**, *B39*, 535.

Table 1. Analytical and Physical Data

compd	color	yield/ %	$\nu_{\max}(\text{CO})^a/\text{cm}^{-1}$	anal. ^{b/c} %	
				C	H
[N(PPh ₃) ₂][6,10-(μ -CO)-6,6,10,10-(CO) ₄ - <i>closo</i> -6,10,1-CO ₂ CB ₇ H ₈] (6)	violet	55	2045 s, 2014 s, 1987 s, 1975 m, 1828 m	56.6 (56.5)	4.2 (4.3)
[N(PPh ₃) ₂][2,3-(μ -CO)-2,2,3,3-(CO) ₄ - <i>closo</i> -2,3,1-CO ₂ CB ₉ H ₁₀] (7)	orange	65	2071 s, 2046 s, 2018 s, 1841 m	54.9 (55.1)	4.4 (4.4)
[PPh ₄][6,7,10-{Co(μ -CO)(CO) ₅ }-7-(μ -H)-6,6-(CO) ₂ - <i>closo</i> -6,1-CO ₂ CB ₈ H ₇] (8b)	dark green	40	2059 s, 2027 s, 2005 s, 1991 br m, 1888 m	40.7 (40.3) ^c	3.6 (3.1)
[6,10-(μ -CO)-6,6,10,10-(CO) ₄ -8-{O(CH ₂) ₄ }- <i>closo</i> -6,10,1-CO ₂ CB ₇ H ₇] (9)	violet	34	2065 s, 2032 s, 2018 s, 1990 m, 1860 m	27.9 (28.3)	3.2 (3.6)
[2,3-(μ -CO)-2,2,3,3-(CO) ₄ -12-{O(CH ₂) ₄ }- <i>closo</i> -2,3,1-CO ₂ CB ₉ H ₉] (10)	orange-red	33	2087 s, 2062 s, 2039 br s, 1866 m	27.2 (26.8)	4.4 (3.8)
[2,3-(μ -CO)-2,2,3,3-(CO) ₄ -12-{O(CH ₂) ₄ PPh ₃ }- <i>closo</i> -2,3,1-CO ₂ CB ₉ H ₉] (11)	orange-red	25	2072 s, 2046 s, 2020 s, 1843 m	43.8 (43.8) ^d	5.0 (4.3)
[7,8,10-{Cu(PPh ₃) ₃ }-7,8-(μ -H)-2,6,10-(μ -CO)-6,6,10,10-(CO) ₄ - <i>closo</i> -6,10,1-CO ₂ CB ₇ H ₆] (12)	violet	29	2071 s, 2039 br s, 1991 m, 1869 m	43.5 (43.5) ^e	3.5 (3.8)
[6,7,8,9,10-{Co ₂ Cu(μ -CO)(CO) ₃ (PPh ₃) ₂ }-6-(μ -CO)-7,8,9-(μ -H)-3-6,6-(CO) ₂ - <i>closo</i> -6,1-CO ₂ CB ₈ H ₅] (13)	brown	22	2059 s, 2023 s, 1974 s, 1921 m, 1799 m	47.2 (46.9) ^d	3.9 (3.5)

^a Measured in CH₂Cl₂; a broad, medium-intensity band observed at ca. 2500–2550 cm⁻¹ in the spectra of all compounds is due to B–H absorptions. ^b Calculated values are given in parentheses. In addition, N: for **6**, 1.8 (1.6); for **7**, 1.7 (1.5). ^c Cocrystallizes with 2.5 molar equiv of CH₂Cl₂. ^d Cocrystallizes with 1.0 molar equiv of CH₂Cl₂. ^e Cocrystallizes with 0.25 molar equiv of C₃H₁₂.

Table 2. ¹H, ¹³C, ¹¹B, and ³¹P NMR Data^a

compd	¹ H ^b / δ	¹³ C ^c / δ	¹¹ B ^d / δ
6 ^e	7.72–7.54 (m, 30H, Ph), 7.28 (br s, 1H, cage CH)	219.9 (vbr, CO), 201.1 (br, CO), 134.1–126.5 (Ph), 116.1 (br, cage C)	28.3, 9.1 (2B), –3.7 (2B), –13.7 (2B)
7 ^e	7.69–7.53 (br m, 30H, Ph), 3.66 (br s, 1H, cage CH)	258.3 (br, μ -CO), 201.2, 195.4 (br \times 2, CO), 133.8–126.5 (Ph), 63.7 (br, cage C)	17.0 (2B), 9.0 (3B), –4.6 (2B), –13.4, –17.4
8a ^e	7.70–7.52 (m, 30H, Ph), 4.34 (br s, 1H, cage CH), –7.01 (br q, <i>J</i> (BH) = 108, 1H, B–H–Co)	213.0, 203.1 (vbr \times 2, CO), 133.8–126.5 (Ph), 49.8 (br, cage C)	71.7 (B(10)), –1.9 (2B), –12.9 (2B), –16.5, –21.5, –30.1
9	7.01 (br s, 1H, cage CH), 4.49 (s, 4H, OCH ₂), 2.27 (s, 4H, CH ₂)	215.9 (vbr, CO), ^f 198.1 (vbr, CO), 110.2 (br, cage C), 83.6 (OCH ₂), 25.6 (CH ₂)	47.9 (B(8)), 11.1 (2B), –3.2 (2B), –16.8 (2B)
10	4.44 (m, 4H, OCH ₂), 3.91 (br s, 1H, cage CH), 2.16 (m, 4H, CH ₂)	252.4 (br, μ -CO), 198.4, 194.3 (br \times 2, CO), 80.4 (OCH ₂), 61.7 (br, cage C), 25.2 (CH ₂)	15.4 (B(12)), 12.9 (2B), 7.8, 4.5 (2B), –8.0 (2B), –16.1
11 ^e	7.53–7.73 (br m, 15H, Ph), 3.94 (br, 1H, cage CH), 3.53 (br, 2H, OCH ₂), 1.87, 1.68, 1.32 (br \times 3, 2H \times 3, CH ₂ \times 3)	258.5 (br, μ -CO), 201.2, 195.2 (br \times 2, CO), 135.2–126.5, 118.7, 117.5 (Ph), 66.5 (OCH ₂), 63.9 (br, cage C), 30.9 (d, <i>J</i> (PC) = 15, PCH ₂), 20.6, 20.4 (PCH ₂ (CH ₂) ₂)	33.4 (B(12)), 17.9 (2B), 6.8 (4B), –7.1, –14.9
12 ^e	7.59–7.53 (br s, 15H, Ph), 7.31 (br, 1H, cage CH)	213.1 (vbr, CO), ^f 197.5 (vbr, CO), 133.8–126.7 (Ph), 117.1 (br, cage C)	12.7, 7.8 (2B), –8.7 (2B), –14.5 (2B)
13 ^e	7.66–7.17 (vbr m, 30H, Ph), 4.48 (br s, 1H, cage CH), –6.43 (br, 1H, B–H–Co)	206.2, ^g 200.4, 199.1 (br \times 3, CO), 136.2–128.7 (Ph), 52.0 (br, cage C)	53.5 (B(10)), –1.0 (2B), –14.8, –20.5 (3B), –37.8

^a Chemical shifts (δ) in ppm, coupling constants (*J*) in Hz, measurements in CD₂Cl₂ at ambient temperatures, except where indicated. ^b Resonances for terminal BH protons occur as broad unresolved signals in the range δ ca. –1 to +3. ^c ¹H-decoupled chemical shifts are positive to high frequency of SiMe₄. ^d ¹H-decoupled chemical shifts are positive to high frequency of BF₃·Et₂O (external); resonances are of unit integral except where indicated. ^e ³¹P{¹H} NMR (positive to high frequency of 85% H₃PO₄ (external)): for **11**, δ 23.7; for **12**, δ 7.7 (br); for **13**, δ 51.1 (br), 3.7 (br). The spectra of compounds **6**, **7**, and **8a** show a singlet resonance at δ 21.7 due to the [N(PPh₃)₂]⁺ cation. ^f Tentative assignment. ^g Measured at 243 K.

associated primarily with one cobalt center or the other, rather than being fluxional between the two. More extensive fluxionality would presumably render all five carbonyl moieties equivalent on the NMR time scale. Notably, the iron-bound CO groups in the related species **2** also appear to remain on their respective iron centers.¹³ The cage carbon atoms appear as typical broad peaks at δ 116.1 (**6**) and 63.7 (**7**) in the ¹³C{¹H} NMR spectra, with a corresponding resonance for their terminal hydrogens at δ 7.28 (**6**) and 3.66 (**7**) in their ¹H NMR spectra. Both compounds also show mirror symmetry in their ¹¹B{¹H} NMR spectra, with **6** giving a 1:2:2:2 pattern of resonances and **7** giving a 2:3 (1 + 2 coincidence):2:1:1 intensity ratio, as required.

In contrast with the formation of **6** and **7**, reaction of [Co₂(CO)₈] with [NEt₄][*closo*-4-CB₈H₉] in THF at room temperature did give a 10-vertex cobaltacarborane cluster (cf. the formation of 10-vertex **3** from the same carborane and [Fe₃(CO)₁₂]¹⁴). Surprisingly, however, the product is the tricoordinated species [6,7,10-{Co(μ -CO)(CO)₅}-7-(μ -H)-6,6-(CO)₂-*closo*-6,1-CO₂CB₈H₇], isolated as the [N(PPh₃)₂]⁺ salt (**8a**) (see Chart 2) following treatment of the reaction mixture with [N(PPh₃)₂]Cl.

Use of [PPh₄][*closo*-4-CB₈H₉] led directly to the corresponding [PPh₄]⁺ salt (**8b**). Although spectroscopic data (Tables 1 and 2; see below) immediately indicated the product to contain a {CB₈} moiety along with at least one cobalt center, as with the anions of **6** and **7** the structure of compounds **8** was initially discovered by X-ray diffraction analysis of **8a**. The results of the latter experiment are shown in Figure 3.

The anion of **8a** consists of a central {*closo*-6,1-CoCB₈} core, similar to the {*closo*-6,1-FeCB₈} core in the ferracarborane **3**,¹⁴ but there the similarity ends. The cluster cobalt vertex (Co(6)) bears two terminal CO ligands, and there is an exo-polyhedral {Co₂(μ -CO)(CO)₄} moiety, within which Co(1)–Co(2) is 2.4838(9) Å. One of the latter cobalt atoms (Co(1)) is also bonded to Co(6) (Co(1)–Co(6) = 2.5779(9) Å). The two exo-polyhedral cobalt centers are also in contact with B(10), which lacks a terminal hydride and instead has a direct σ bond to Co(2). As B(10) is also adjacent to the cluster cobalt vertex, it is thus within bonding distance of all three metals (Co(1)–B(10) = 2.182(3) Å, Co(2)–B(10) = 2.097(3) Å, and Co(6)–B(10) = 2.021(3) Å), with this {BCO₃} unit having an overall “butterfly” shape. An additional feature of the structure is a

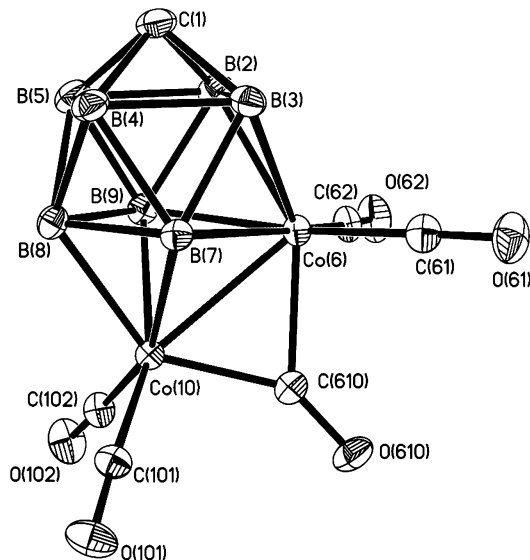


Figure 1. Perspective view of the anion of compound **6** showing the crystallographic labeling scheme. In this and subsequent figures, thermal ellipsoids are drawn with 40% probability, and for clarity only chemically significant hydrogen atoms are shown. Selected internuclear distances (Å) and angles (deg): Co(6)–Co(10) = 2.4331(3), Co(6)–B(2) = 2.1385(17), Co(6)–B(3) = 2.1289(16), Co(6)–B(7) = 2.1970(14), Co(6)–B(9) = 2.1845(16), Co(6)–C(61) = 1.7718(15), Co(6)–C(62) = 1.7570(13), Co(6)–C(610) = 1.9987(14), Co(10)–B(7) = 2.1210(14), Co(10)–B(8) = 2.0853(16), Co(10)–B(9) = 2.1311(15), Co(10)–C(101) = 1.7649(13), Co(10)–C(102) = 1.7686(14), Co(10)–C(610) = 1.8390(14); O(610)–C(610)–Co(10) = 146.30(12), O(610)–C(610)–Co(6) = 135.12(12).

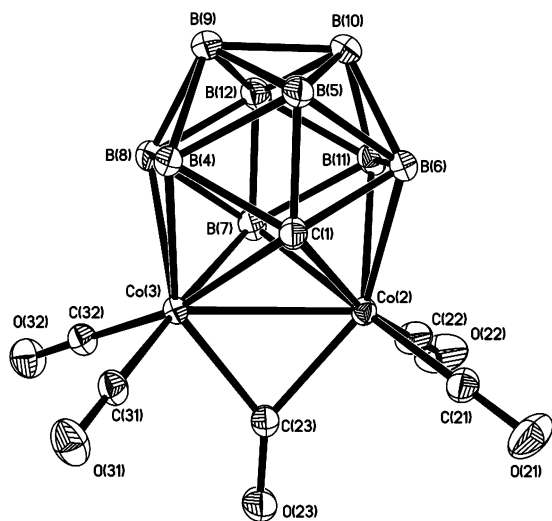


Figure 2. Perspective view of the anion of compound **7** showing the crystallographic labeling scheme. Selected internuclear distances (Å) and angles (deg): Co(2)–Co(3) = 2.4396(2), Co(2)–C(1) = 2.1305(11), Co(2)–B(6) = 2.1226(13), Co(2)–B(7) = 2.1769(14), Co(2)–B(11) = 2.1381(14), Co(2)–C(21) = 1.7878(13), Co(2)–C(22) = 1.7542(14), Co(2)–C(23) = 1.9108(13), Co(3)–C(31) = 1.7892(13), Co(3)–C(32) = 1.7595(13), Co(3)–C(23) = 1.9156(12), Co(3)–C(1) = 2.1167(12), Co(3)–B(4) = 2.1220(13), Co(3)–B(7) = 2.1838(14), Co(3)–B(8) = 2.1350(14); O(23)–C(23)–Co(2) = 140.59(11), O(23)–C(23)–Co(3) = 139.99(11).

three-center, two-electron agostic-type B–H→Co bond involving Co(1) and B(7) (Co(1)⋯B(7) = 2.165(3) Å, Co(1)–H(7) = 1.75(3) Å).

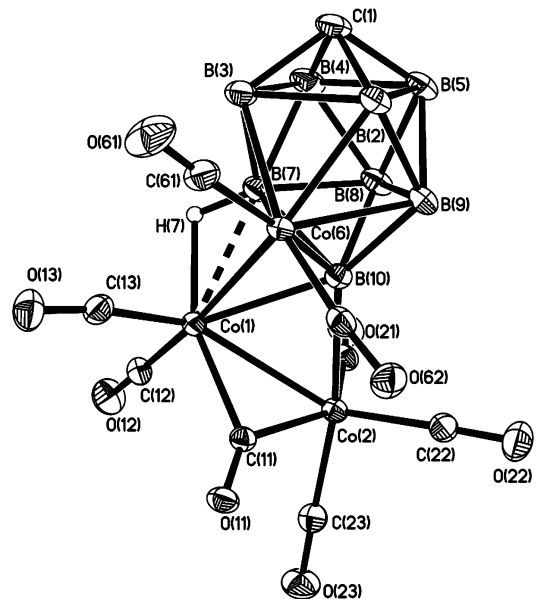


Figure 3. Perspective view of the anion of compound **8a** showing the crystallographic labeling scheme. Selected internuclear distances (Å) and angles (deg): Co(1)–Co(2) = 2.4838(9), Co(1)–Co(6) = 2.5779(9), Co(6)–B(2) = 2.141(3), Co(6)–B(3) = 2.153(3), Co(6)–B(7) = 2.141(3), Co(6)–B(9) = 2.203(3), Co(6)–B(10) = 2.021(3), Co(6)–C(61) = 1.765(3), Co(6)–C(62) = 1.764(2), Co(1)–H(7) = 1.75(3), Co(1)⋯B(7) = 2.165(3), Co(1)–B(10) = 2.182(3), Co(2)–B(10) = 2.097(3), Co(1)–C(11) = 1.897(2), Co(1)–C(12) = 1.785(3), Co(1)–C(13) = 1.773(3), Co(2)–C(11) = 1.916(2), Co(2)–C(21) = 1.796(2), Co(2)–C(22) = 1.773(3), Co(2)–C(23) = 1.790(3); Co(2)–Co(1)–Co(6) = 92.80(3), B(10)–Co(6)–Co(1) = 55.05(8), Co(2)–B(10)–Co(1) = 70.93(9), Co(6)–B(10)–Co(1) = 75.55(9), Co(6)–B(10)–Co(2) = 125.76(13), B(10)–Co(1)–Co(2) = 52.94(7), B(10)–Co(2)–Co(1) = 56.12(7), B(10)–Co(1)–Co(6) = 49.41(7).

The IR spectra of compounds **8** displayed four strong terminal CO stretching bands (ν_{\max} 2059, 2027, 2005, and 1991 cm^{-1}), of which that to lowest frequency was rather broad, along with a medium-intensity band at ν_{\max} 1888 cm^{-1} for the bridging CO group. Although the bridging carbonyl has a slightly higher frequency than in **6** and **7**, these data for **8** are otherwise comparable to those for **6** and **7**. The ^1H NMR spectrum of **8a** shows a diagnostic¹⁸ broad quartet at δ –7.01 ($J(\text{BH}) \approx 108$ Hz) for the B–H→Co agostic-type bond, with a broad singlet at δ 4.34 for the cage {CH} unit. The latter also appears as a broad resonance (δ 49.8) in the $^{13}\text{C}\{^1\text{H}\}$ NMR spectrum, while the eight CO ligands give rise to only two very broad signals (δ 213.0 and 203.1), indicating considerable fluxionality for these moieties. In its $^{11}\text{B}\{^1\text{H}\}$ NMR spectrum compound **8a** shows six signals, of which one is at δ 71.7 and the remaining five occur between δ –1.9 and –31.1, with the six being in the ratio 1:2:2:1:1:1. The very low-field resonance (δ 71.7) remains a singlet upon retention of proton coupling and is assigned as B(10); such a chemical shift is typical for a boron atom involved in a direct B–transition-metal σ bond.¹⁸ Although the salts **8** are reasonably stable when stored under an inert atmosphere in the solid state and survive in solution for several days, NMR analysis indicates that they entirely decompose after 1 month in solution, even when stored at –30 °C.

The formation of the anions of compounds **6** and **7** may be viewed as successive oxidative insertion of two {Co(CO)₂}

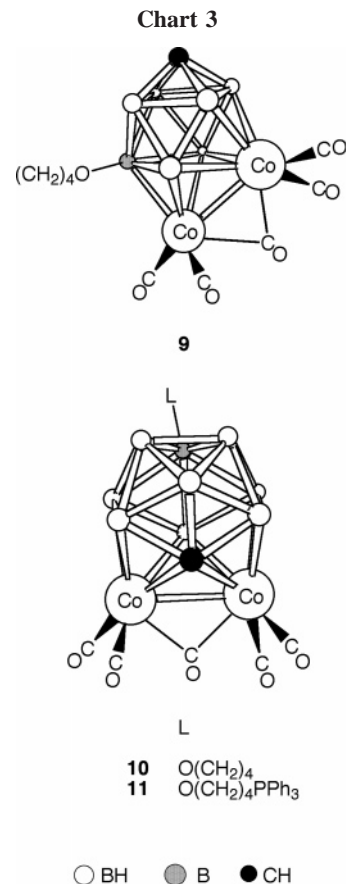
(18) Brew, S. A.; Stone, F. G. A. *Adv. Organomet. Chem.* **1993**, *35*, 135.

fragments into the carborane precursor, analogous to the generation of **1** and then **2** from [*closo*-1-CB₇H₈][−] by sequential incorporation of two {Fe(CO)₃} moieties.¹³ A consideration of the formal charge (−5) on the carborane ligand in the anions of **6** and **7** indicates that both cobalt centers must formally be in the +2 oxidation state, like the iron centers in **1** and **2**. This would imply 17-electron configurations for each cobalt, and hence the additional bridging CO ligand completes an electron count of 18 for each metal center. In parallel with this, insertion of a single {Co(CO)₂} unit into [*closo*-4-CB₈H₉][−] would be analogous to the formation of **3** and again a Co²⁺ valency may be invoked. However, the resulting 10-vertex {(CO)₂CoCB₈H₉}[−] unit (cf. the cluster core of compounds **8**) would not be expected to readily accept another metal vertex, given the known stability of 10-vertex clusters.¹⁹ Instead, the 17-electron configuration in this case is relieved by the additional exo-polyhedral cobalt unit and concomitant loss of the terminal hydrogen atom formerly bonded to B(10), presumably as 1/2H₂. The latter one-electron process returns the three cobalt atoms to an even electron count, consistent with the diamagnetism of the complex. Various canonical forms can be drawn, and oxidation states ranging from 0 to +3 can be invoked for the three metal centers to account for the structure of this complex, but a more detailed picture is beyond this qualitative description. We note, however, that the similarity in CO stretching frequencies for all three of the anions of compounds **6–8** implies that a model involving a +3 oxidation state in the anion of compounds **8** is probably not appropriate, as this would likely cause the CO frequencies to be somewhat higher.

It was of interest to perform some preliminary reactivity studies upon the cobalt-monocarbollide complexes **6–8**. As all three retain a negative charge, it seemed likely that they would be resistant to substitution of their CO ligands by other donor molecules such as phosphines, isocyanides, or alkynes.⁷ This proved to be the case in practice, as no reaction was observed between **6** or **7** and various donors (e.g., PPh₃, alkynes), even in the presence of Me₃NO and with elevated reaction temperatures. Attempts to replace a CO group by [NO]⁺ using [NO]-[BF₄][−] also were unsuccessful. In the case of compounds **8**, the anion was somewhat too fragile and typically decomposed under such conditions, with [Co₄(CO)₁₂] observed among other, unidentified products.

The anionic nature of these species, however, does make them attractive substrates for reactions with electrophiles. Thus, in an initial investigation it was found that treatment of **6** or **7** with CF₃SO₃Me in CH₂Cl₂–THF (1:1) resulted in the Me⁺ electrophile behaving as a hydride abstraction agent, with a terminal boron-bound H[−] unit being replaced by a THF molecule to give the neutral, zwitterionic species [6,10-(μ-CO)-6,6,10,10-(CO)₄-8-{O(CH₂)₄}-*closo*-6,10,1-CO₂CB₇H₇] (**9**) and [2,3-(μ-CO)-2,2,3,3-(CO)₄-12-{O(CH₂)₄}-*closo*-2,3,1-CO₂-CB₉H₉] (**10**), respectively (see Chart 3). Such hydride abstraction reactions to form charge-compensated species have multiple precedents among other metal–monocarbollide anions.^{6,7}

The identities of both of compounds **9** and **10**, and in particular the sites of THF substitution, were confirmed by X-ray diffraction studies. The results of these experiments are shown in Figures 4 and 5, respectively. Both molecules retain the overall geometry of their parent anions and in particular still have carbonyl-bridged Co–Co bonds. In compound **9**, this metal–metal bond (Co(6)–Co(10) = 2.4071(14) Å) is significantly shorter than that in the precursor **6**, while in compound **10** the corresponding distance (Co(2)–Co(3) = 2.4397(3) Å



is essentially identical with that in **7**. For **9** the THF substituent is bonded to B(8), which is adjacent to one of the metal centers, and is also the vertex where similar substitution occurs in reactions of compound **2**.¹³ In contrast, for compound **10** the THF moiety is attached to B(12), which is distant from both metal centers. In both cases, however, the site of boron substitution is as far as possible from the cage carbon vertex.

Spectroscopic data for **9** and **10** are collected in Tables 1 and 2. As was evident in the structure determinations, both

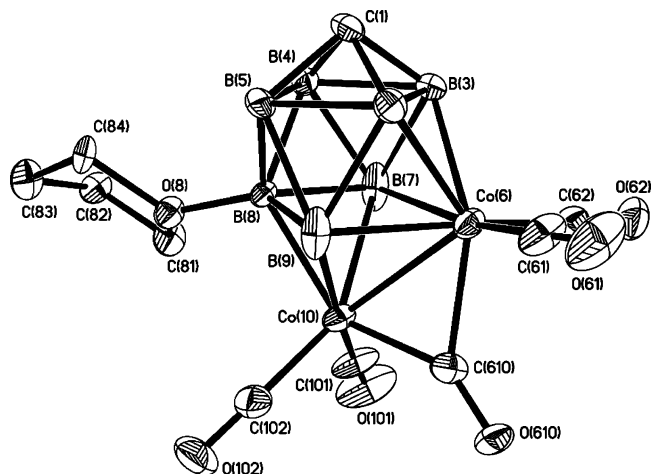


Figure 4. Perspective view of compound **9** showing the crystallographic labeling scheme. Selected internuclear distances (Å) and angles (deg): Co(6)–Co(10) = 2.4071(14), B(2)–Co(6) = 2.128(9), B(3)–Co(6) = 2.154(9), B(7)–Co(6) = 2.206(8), B(9)–Co(6) = 2.181(8), B(7)–Co(10) = 2.122(10), B(8)–Co(10) = 2.058(7), B(9)–Co(10) = 2.014(10), Co(6)–C(610) = 2.004(8), Co(10)–C(610) = 1.885(8), B(8)–O(8) = 1.537(9); O(610)–C(610)–Co(6) = 136.3(7), O(610)–C(610)–Co(10) = 146.6(7), O(8)–B(8)–Co(10) = 109.9(5).

(19) Schleyer, P. v. R.; Najafian, K. *Inorg. Chem.* **1998**, *37*, 3454.

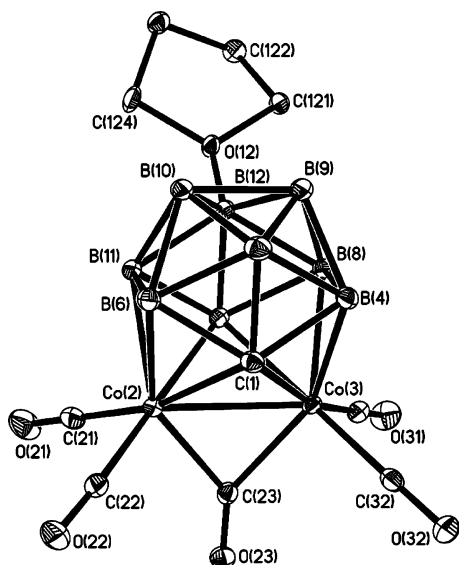


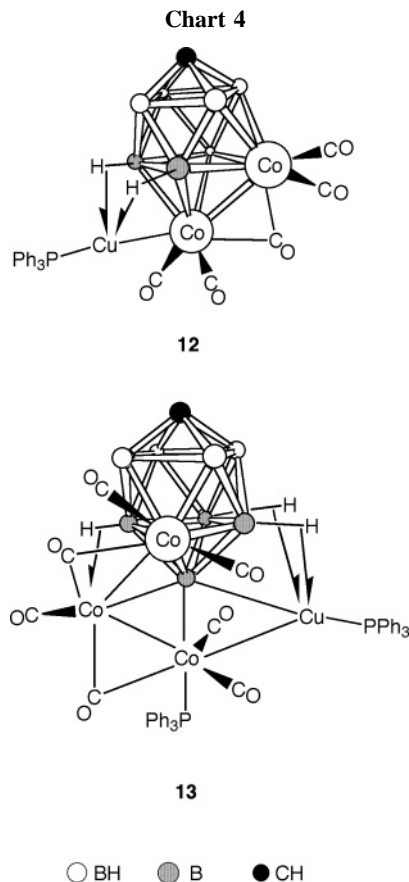
Figure 5. Perspective view of compound **10** showing the crystallographic labeling scheme. Selected internuclear distances (Å) and angles (deg): Co(2)–Co(3) = 2.4397(3), Co(2)–C(21) = 1.7648(19), Co(2)–C(22) = 1.8018(18), Co(2)–C(23) = 1.9239(16), Co(2)–C(1) = 2.1200(17), Co(2)–B(6) = 2.1119(19), Co(2)–B(7) = 2.1774(19), Co(2)–B(11) = 2.1289(18), Co(3)–C(1) = 2.1067(16), Co(3)–B(4) = 2.1143(19), Co(3)–B(7) = 2.1673(18), Co(3)–B(8) = 2.1356(18), Co(3)–C(23) = 1.9198(17), Co(3)–C(31) = 1.7612(18), Co(3)–C(32) = 1.8057(17), B(12)–O(12) = 1.510(2); O(23)–C(23)–Co(2) = 140.41(14), O(23)–C(23)–Co(3) = 140.69(14).

compounds retain the molecular mirror symmetry of their precursors. Thus, the $^{11}\text{B}\{^1\text{H}\}$ NMR spectrum of **9** shows four resonances in the ratio 1:2:2:2, while that of **10** has six peaks in the ratio 1:2:1:2:2:1. In both cases, the highest frequency signal (δ 47.9 (**9**) and 15.4 (**10**)) remains a singlet in a fully proton-coupled spectrum and, therefore, is assigned to the boron atom bearing the THF substituent. The ^1H and $^{13}\text{C}\{^1\text{H}\}$ NMR spectra show signals in the expected positions and appropriate ratios for the THF groups and the cage $\{\text{CH}\}$ vertices.

It was expected that the neutral molecule **10** would be more susceptible to CO substitution than the precursor **7**. However, treatment of **10** with PPh_3 instead resulted in nucleophilic attack upon the THF unit. In **10**, a positive center is formally located upon the three-coordinate oxygen atom and the phosphine attack occurred at a methylene unit adjacent to this site, resulting in ring opening and formation of the complex $[2,3-(\mu\text{-CO})\text{-}2,2,3,3\text{-}(\text{CO})_4\text{-}12\text{-}\{\text{O}(\text{CH}_2)_4\text{PPh}_3\}\text{-}closo\text{-}2,3,1\text{-}\text{Co}_2\text{CB}_9\text{H}_9]$ (**11**). Analogous reactions have been observed in a variety of other systems.²⁰ Data characterizing compound **11** are given in Tables 1 and 2 and as expected bear some similarity to those for **10**. Additional ^1H and $^{13}\text{C}\{^1\text{H}\}$ NMR signals are seen for the PPh_3 unit, and the four CH_2 units of the former THF molecule now each produce separate resonances in both spectra, with the resonance for the methylene carbon atom that is directly bonded to phosphorus showing doublet structure (δ 30.9; $J(\text{PC}) = 15$ Hz). The phosphorus center itself gives rise to a singlet in the $^{31}\text{P}\{^1\text{H}\}$ NMR spectrum at δ 23.7.

In addition to reactions with nucleophiles such as Me^+ as discussed above, it is also known that anionic metallacarboranes

(20) Examples include: Mullica, D. F.; Sappenfield, E. L.; Stone, F. G. A.; Woollam, S. F. *Organometallics* **1994**, *13*, 157. Du, S.; Franken, A.; Jelliss, P. A.; Kautz, J. A.; Stone, F. G. A.; Yu, P.-Y. *J. Chem. Soc., Dalton Trans.* **2001**, 1846. McGrath, T. D.; Stone, F. G. A.; Sukcharoenphon, K. *J. Cluster Sci.* **2005**, *16*, 201.



readily react with transition-metal cations to afford bi- or polymetallic species.^{7,21} As the cobalt–monocarborane complexes of compounds **6–8** are monoanionic, it was decided to investigate their reactivity with a monocationic fragment, specifically $\{\text{Cu}(\text{PPh}_3)\}^+$, in the hope of obtaining neutral copper–cobalt polymetallic products. Both **6** and **8** did indeed form $\{\text{Cu}\text{-Co}_2\text{CB}_7\}$ and $\{\text{Cu}\text{-Co}_3\text{CB}_8\}$ derivatives, respectively, upon treatment with $[\text{CuCl}(\text{PPh}_3)]_4$ and $\text{Ti}[\text{PF}_6]$, the latter being added to remove Cl^- as insoluble TiCl . However, very surprisingly, compound **7** failed to yield any corresponding $\{\text{Cu}\text{-Co}_2\text{CB}_9\}$ product.

The reaction of **6** with the copper moiety afforded the trimetallic species $[7,8,10\text{-}\{\text{Cu}(\text{PPh}_3)\}\text{-}7,8\text{-}(\mu\text{-H})_2\text{-}6,10\text{-}(\mu\text{-CO})\text{-}6,6,10,10\text{-}(\text{CO})_4\text{-}closo\text{-}6,10,1\text{-}\text{Co}_2\text{CB}_7\text{H}_6]$ (**12**) (see Chart 4), for which characterizing data are given in Tables 1 and 2. Although crystals of **12** were available and X-ray diffraction studies were performed, any data collected were always of very poor quality, as a result of apparently severe twinning. Thus, although a solution could be obtained and the heavy-atom connectivity pattern and site of attachment of the copper unit were found to be those shown in Chart 4, further refinement was not possible.

Spectroscopic data for compound **12** are suggestive of a symmetric structure, with the $^{11}\text{B}\{^1\text{H}\}$ NMR data showing a 1:2:2:2 intensity pattern, similar to that of the parent, suggesting that the exo-polyhedral copper fragment is fluxional with respect to the cluster surface. Similar behavior was noted in the related $\{\text{Cu}(\text{PPh}_3)\}^+$ derivatives of **1**, **2**, and **4**.^{13,14} Likewise, such processes mean that no signals for protons involved in $\text{B}\text{-H}\text{-Cu}$ bridges are seen in the ^1H NMR spectrum of **12**. This is typical of species of this type, as the fluxional processes appear to be

(21) Other examples include: Ellis, D. D.; Jelliss, P. A.; Stone, F. G. A. *Organometallics* **1999**, *18*, 4982. Hodson, B. E.; McGrath, T. D.; Stone, F. G. A. *Organometallics* **2005**, *24*, 1638.

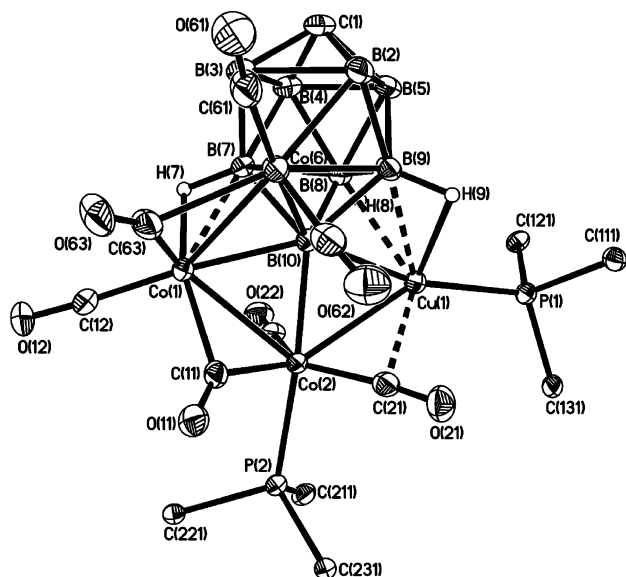


Figure 6. Perspective view of compound **13** showing the crystallographic labeling scheme. For clarity only the ipso carbon atoms of phenyl rings are shown. Selected internuclear distances (Å) and angles (deg): Co(1)–Co(2) = 2.5731(10), Co(1)–Co(6) = 2.5833(10), Co(1)···B(7) = 2.164(4), Co(1)–H(7) = 1.84(3), Co(1)–B(10) = 2.154(3), Co(2)–B(10) = 2.123(3), Co(2)–Cu(1) = 2.5049(9), C(21)···Cu(1) = 2.281(3), Co(6)–B(2) = 2.170(4), Co(6)–B(3) = 2.185(5), Co(6)–B(7) = 2.199(4), Co(6)–B(9) = 2.199(3), Co(6)–B(10) = 2.048(3), B(8)···Cu(1) = 2.285(3), B(9)···Cu(1) = 2.386(3), B(10)–Cu(1) = 2.184(3); Co(2)–Co(1)–Co(6) = 94.85(2), B(10)–Co(1)–Co(2) = 52.47(9), B(10)–Co(1)–Co(6) = 50.23(9), B(10)–Co(2)–Cu(1) = 55.58(9), B(10)–Co(2)–Co(1) = 53.56(9), Cu(1)–Co(2)–Co(1) = 108.588(19), B(10)–Co(6)–Co(1) = 53.93(9), Co(2)–B(10)–Co(1) = 73.98(11), Co(6)–B(10)–Co(1) = 75.84(11), Co(6)–B(10)–Co(2) = 131.12(18), Co(1)–B(10)–Cu(1) = 143.88(16), Co(2)–B(10)–Cu(1) = 71.12(10), Co(6)–B(10)–Cu(1) = 136.16(17), B(10)–Cu(1)–Co(2) = 53.31(9).

fast on the NMR time scale, even at lower temperatures.²² Moreover, such protons would in any event give rise to very broad peaks even in a static structure, as a consequence of the adjacent quadrupolar boron and copper nuclei.

In contrast with the relatively straightforward nature of compound **12**, the copper–phosphine derivative obtained from compounds **8** is rather more than a simple adduct. The product is the tetrametallic species [6,7,8,9,10- $\{Co_2Cu(\mu-CO)(CO)_3-(PPh_3)_2\}$ -6-($\mu-CO$)-7,8,9-($\mu-H$)-3,6,6-(CO)₂-*closo*-6,1-CoCB₈H₅] (**13**). Although initial IR and NMR spectroscopic data (Tables 1 and 2; see below) confirmed the presence of the expected copper–phosphine, cobalt–carbonyl, and carborane components within the complex, the precise nature of the species was only established following an X-ray diffraction experiment. The structure so determined is shown in Figure 6.

Compound **13** retains the {*closo*-6,1-CoCB₈} core of the parent, along with the two exo-polyhedral cobalt centers, and has gained an exo-polyhedral copper moiety. However, each of the three cobalt atoms has undergone some modification in its coordination sphere. The cluster cobalt vertex (Co(6)) still has two terminal CO ligands, as in **8a**, but now also is bonded to a bridging CO group that is also attached to Co(1). In addition

to that bridging carbonyl, Co(1) now carries only one terminal CO (compared with two in **8a**), but the Co(1)–Co(2) bond retains a μ -CO group, and the B(7)–H(7)→Co(1) linkage also remains, both of these last two features also being found in **8a**. Finally, one of the three CO ligands formerly bonded to Co(2) has been replaced by a PPh₃ group; evidently the attachment of the copper unit, forming a neutral species, sufficiently labilizes CO ligands toward substitution. That last cobalt atom (Co(2)) is still σ bonded to B(10) and now also is connected to the exo-polyhedral copper atom. The copper center is itself also involved in agostic-type B–H→Cu bridges involving BH(8) and BH(9) and in addition is approached by one of the CO ligands bonded to Co(2). All of these last three interactions, however, are rather weak, as demonstrated by rather long Cu···B distances (Cu(1)···B(8) = 2.285(3) Å, Cu(1)···B(9) = 2.386(3) Å), and by a long Cu···C distance (Cu(1)···C(21) = 2.281(3) Å) with the Co(2)–C(21)–O(21) angle (171.1(3)°) only slightly distorted from linearity. Notably, the copper is also adjacent to B(10), so that this atom is now within bonding range of four metal atoms (Co(1)–B(10) = 2.154(3) Å, Co(2)–B(10) = 2.123(3) Å, Co(6)–B(10) = 2.048(3) Å, and Cu(1)–B(10) = 2.184(3) Å). As with the anion of compounds **8**, however, the precise details of the metal···metal and metal···cage interactions in **13** are clearly complex, and various representations could account for the observed structure. The bonding is probably highly delocalized, and again, a full description is beyond the present discussion.

Spectroscopic data for **13** were, as already mentioned, consistent with the solid-state structure. The two different types of PPh₃ units gave rise to two broad signals in the ³¹P{¹H} NMR spectrum, at δ 51.1 and 3.7, these being in typical positions for such a ligand bonded to cobalt and copper, respectively. The ¹¹B{¹H} NMR spectrum was quite broad and consists of only five resonances in the ratio 1:2:1:3:1, but the peaks of integral greater than unity are due to coincidences in this asymmetric molecule. The highest frequency boron resonance (δ 53.5) remains a singlet upon retention of proton coupling and is assigned to B(10). Notably, this peak is almost 20 ppm more shielded in comparison with that in compounds **8**, possibly a consequence of the attachment of the additional metal center and/or of the transoid PPh₃ ligand now bonded to Co(2). Only three broad signals are seen for CO groups in the ¹³C{¹H} NMR spectrum, even at 243 K, indicating that these ligands remain fluxional, as is not unexpected. The same spectrum also shows peaks for the Ph groups and a broad resonance at δ 52.0 for the cage carbon atom, close to the corresponding data for **8a**. The cluster CH proton resonates at δ 4.48 in the ¹H NMR spectrum, likewise similar to the chemical shift for the same unit in **8a**, while this spectrum also reveals a broad peak at δ –6.43 that is assigned to the B–H→Co unit and is slightly deshielded compared to that in **8a**. Like compound **12**, no signal was observed for the protons involved in the B–H→Cu linkages.²²

It should be noted in passing that all three of the compounds **6**–**8** also appeared to give cobaltcarborane products upon reaction with sources of {M(PPh₃)⁺} (M = Ag, Au), of which those obtained from **8** were perhaps the most stable and appeared possibly to be monocobalt species. Consistent with the latter observation, [Co₄(CO)₁₂] was often also observed as a side product in such reactions. However, all of the metallacarboranes formed in these reactions have thus far defied complete characterization and our efforts continue in this direction.

Conclusion

We have prepared and fully characterized the new cobaltcarboranes **6**–**8**, which are formed from reactions of [Co₂(CO)₈]

(22) (a) Jeffery, J. C.; Ruiz, M. A.; Sherwood, P.; Stone, F. G. A. *J. Chem. Soc., Dalton Trans.* **1989**, 1845. (b) Carr, N.; Gimeno, M. C.; Goldberg, J. E.; Pilotti, M. U.; Stone, F. G. A.; Topaloglu, I. *J. Chem. Soc., Dalton Trans.* **1990**, 2253. (c) Jeffery, J. C.; Jelliss, P. A.; Stone, F. G. A. *J. Chem. Soc., Dalton Trans.* **1993**, 1073. (d) Jeffery, J. C.; Jelliss, P. A.; Rees, L. H.; Stone, F. G. A. *Organometallics* **1998**, *17*, 2258.

Table 3. Crystallographic Data for Compounds 6, 7, 8a, 9, 10, and 13

	6	7	8a	9	10·0.5CH ₂ Cl ₂	13 ^a
formula	C ₄₂ H ₃₈ B ₇ Co ₂ -NO ₅ P ₂	C ₄₂ H ₄₀ B ₉ Co ₂ -NO ₅ P ₂	C ₄₅ H ₃₈ B ₈ Co ₃ -NO ₈ P ₂	C ₁₀ H ₁₅ B ₇ Co ₂ O ₆	C _{10.5} H ₁₈ B ₉ Cl-Co ₂ O ₆	C ₄₄ H ₃₈ B ₈ Co ₃ Cu-O ₇ P ₂
fw	892.20	915.84	1045.97	424.75	490.85	1067.49
space group	<i>P</i> $\bar{1}$	<i>P</i> $\bar{1}$	<i>P</i> 2 ₁ / <i>n</i>	<i>P</i> <i>bca</i>	<i>P</i> $\bar{1}$	<i>P</i> 2 ₁ / <i>n</i>
<i>a</i> /Å	11.5563(6)	11.4458(3)	16.335(8)	13.8830(8)	7.7050(2)	13.317(5)
<i>b</i> /Å	12.7164(7)	13.9304(5)	10.146(4)	14.5367(7)	9.2280(2)	17.027(6)
<i>c</i> /Å	15.1804(9)	14.3501(5)	28.834(13)	17.2427(8)	13.9476(3)	21.905(8)
α /deg	109.367(3)	73.497(2)	90	90	94.902(1)	90
β /deg	90.463(3)	89.679(2)	105.856(10)	90	90.281(1)	91.534(10)
γ /deg	97.224(3)	79.609(2)	90	90	100.842(1)	90
<i>V</i> /Å ³	2084.9(2)	2155.28(12)	4597(4)	3479.8(3)	970.21(4)	4965(3)
<i>Z</i>	2	2	4	8	2	4
ρ_{calcd} /g cm ⁻³	1.421	1.411	1.511	1.622	1.680	1.428
μ (Mo K α)/mm ⁻¹	0.919	0.890	1.194	1.928	1.873	1.518
no. of rflns measd	80 335	59 650	52 292	22 735	14 163	52 626
no. of indep rflns	15 254	15 774	14 672	3486	4426	10 918
<i>R</i> _{int}	0.0381	0.0333	0.0600	0.0877	0.0250	0.0568
wR2, R1 ^b (all data)	0.0910, 0.0517	0.0897, 0.0421	0.1044, 0.0776	0.2250, 0.1133	0.0628, 0.0304	0.1019, 0.0686
wR2, R1 (obsd ^c data)	0.0850, 0.0334	0.0857, 0.0315	0.0898, 0.0436	0.2005, 0.0784	0.0600, 0.0256	0.0896, 0.0411

^a The crystals contained an unidentified solvate (see text). The formula and the values for fw, ρ_{calcd} , and μ given here ignore the presence of this solvate.
^b wR2 = $[\sum\{w(F_o^2 - F_c^2)^2\}/\sum w(F_o^2)^2]^{1/2}$; R1 = $\sum||F_o| - |F_c||/\sum|F_o|$. ^c $F_o > 4\sigma(F_o)$.

with {CB₇}, {CB₉}, and {CB₈} carborane substrates, respectively. Compounds **6** and **7** constitute a pair of related dicobalt species, of which the 12-vertex complex **7** has some counterparts in cobaltaborane chemistry, whereas the tricobalt–monocarboride anion in compounds **8** has a very surprising and—to our knowledge—unprecedented structure. Some preliminary studies upon the reactivity of these clusters with electrophilic reagents have been performed. Both **6** and **7** undergo hydride abstraction by Me⁺ in the presence of THF to afford neutral and zwitterionic B-THF-substituted complexes, while **6** also forms a CuCo₂ trimetallic product upon treatment with {Cu(PPh₃)⁺. In parallel with the latter, the reaction of **8** with {Cu(PPh₃)⁺ gives a CuCo₃ tetrametallic complex, also of unprecedented structure. It will be of interest in the future to determine the nature of the other products obtained from reaction of **8** with {M(PPh₃)⁺ fragments and, indeed, to investigate further whether all of these cobaltacarboranes undergo reactions with the many other cationic transition-element moieties that are available.^{7,21}

Experimental Section

General Considerations. Reactions were carried out under an atmosphere of dry, oxygen-free dinitrogen using standard Schlenk techniques. Solvents were distilled from appropriate drying reagents under nitrogen prior to use. Petroleum ether refers to that fraction of boiling point 40–60 °C. Chromatography columns (ca. 15 cm in length and ca. 2 cm in diameter) were packed with silica gel (Acros, 60–200 mesh). Celite pads used for filtration were typically ca. 3 cm in depth and ca. 2 cm in diameter. NMR spectra were recorded at the following frequencies (MHz): ¹H, 360.1; ¹³C, 90.6; ¹¹B, 115.5; ³¹P, 145.8. The reagents [NBuⁿ]₄[*closo*-1-CB₇H₈],⁵ [NEt₄][*closo*-4-CB₈H₉],⁵ [PPh₄][*closo*-4-CB₈H₉],⁵ [NEt₄][*arachno*-6-CB₉H₁₄],^{1,5} and [CuCl(PPh₃)₄]²³ were prepared according to the literature. All other materials were used as received.

Reaction of [Co₂(CO)₈] with Monocarborane Anions. (i) To a THF (5 mL) solution of [NBuⁿ]₄[*closo*-1-CB₇H₈] (0.170 g, 0.50 mmol) was added [Co₂(CO)₈] (0.171 g, 0.50 mmol). The mixture was stirred for 5 h, and [N(PPh₃)₂]Cl (0.287 g, 0.50 mmol) was added. Stirring was continued overnight, and then the solution was concentrated to ca. 1 mL and chromatographed. Elution with CH₂Cl₂–petroleum ether (4:1) removed a violet band which, after evaporation of solvent in vacuo, gave [N(PPh₃)₂][6,10-(μ -CO)-6,6,-

10,10-(CO)₄-*closo*-6,10,1-CO₂CB₇H₈] (**6**; 0.245 g) as a violet microcrystalline solid.

(ii) By an analogous procedure, [NEt₄][*arachno*-6-CB₉H₁₄] (0.111 g, 0.43 mmol) and [Co₂(CO)₈] (0.175 g, 0.51 mmol), stirred for 5 h in THF (5 mL), followed by [N(PPh₃)₂]Cl (0.250 g, 0.44 mmol) addition, stirring for a further 16 h, and then workup as above, afforded [N(PPh₃)₂][2,3-(μ -CO)-2,2,3,3-(CO)₄-*closo*-2,3,1-CO₂-CB₉H₁₀] (**7**; 0.259 g) as an orange-red powder.

(iii) Similarly, [NEt₄][*closo*-4-CB₈H₉] (0.155 g, 0.64 mmol) and [Co₂(CO)₈] (0.376 g, 1.10 mmol) were stirred at room temperature in THF (5 mL) for 2 h, followed by addition of [N(PPh₃)₂]Cl (0.367 g, 0.64 mmol) and stirring for a further 2 h. Workup as above gave [N(PPh₃)₂][6,7,10-{Co₂(μ -CO)(CO)₅}-7-(μ -H)-6,6-(CO)₂-*closo*-6,1-CO₂CB₈H₇] (**8a**; 0.196 g, 39%) as deep green microcrystals. The [PPh₄]⁺ salt **8b** (yield 0.216 g) was synthesized by a related procedure, using [PPh₄][*closo*-4-CB₈H₉] as the starting carborane.

Synthesis of Zwitterionic B-Substituted Compounds. (i) Compound **6** (0.263 g, 0.29 mmol) was dissolved in CH₂Cl₂–THF (1:1, 20 mL), and CF₃SO₃Me (0.15 mL) was added. After it was stirred overnight, the mixture was evaporated to dryness and the residue was redissolved in CH₂Cl₂ (1 mL) and chromatographed. Elution with CH₂Cl₂–petroleum ether (1:1) gave a violet band which, after evaporation of solvent in vacuo, afforded [6,10-(μ -CO)-6,6,10,10-(CO)₄-8-{O(CH₂)₄}-*closo*-6,10,1-CO₂CB₇H₇] (**9**; 0.043 g) as violet microcrystals.

(ii) By a similar procedure, from compound **7** (0.160 g, 0.17 mmol) and CF₃SO₃Me (0.15 mL) was obtained [2,3-(μ -CO)-2,2,3,3-(CO)₄-12-{O(CH₂)₄}-*closo*-2,3,1-CO₂CB₉H₉] (**10**; 0.025 g) as a microcrystalline orange-red solid.

(iii) Compound **10** (0.050 g, 0.11 mmol) and PPh₃ (0.030 g, 0.11 mmol) were stirred overnight in CH₂Cl₂ (10 mL). Chromatographic workup as above, but with CH₂Cl₂–THF (9:1) as eluent, gave [2,3-(μ -CO)-2,2,3,3-(CO)₄-12-{O(CH₂)₄}-*closo*-2,3,1-CO₂CB₉H₉] (**11**; 0.021 g) as an orange-red powder.

Reactions with {Cu(PPh₃)⁺. (i) Compound **6** (0.252 g, 0.28 mmol), [CuCl(PPh₃)₄] (0.102 g, 0.07 mmol), and Tl[PF₆] (0.098 g, 0.28 mmol) were stirred in CH₂Cl₂ (10 mL) for 2 h. After filtration (Celite), the filtrate was concentrated to ca. 2 mL and chromatographed. Elution with CH₂Cl₂–petroleum ether (1:1) gave a violet band which, after evaporation of solvent in vacuo, gave [7,8,10-{Cu(PPh₃)₂}-7,8-(μ -H)-6,10-(μ -CO)-6,6,10,10-(CO)₄-*closo*-6,10,1-CO₂CB₇H₆] (**12**; 0.055 g) as violet microcrystals.

(ii) Similarly, compound **8a** (0.251 g, 0.24 mmol), [CuCl(PPh₃)₄] (0.090 g, 0.06 mmol) and Tl[PF₆] (0.089 g, 0.26 mmol) afforded [6,7,8,9,10-{Co₂Cu(μ -CO)(CO)₅(PPh₃)₂}-6-(μ -CO)-7,8,9-(μ -H)-3-

6,6-(CO)₂-*closo*-6,1-CoC₈H₅] (**13**; 0.058 g) as a brown microcrystalline solid.

Compound **13** appeared to be very unstable in solution, and thus longer reaction times drastically reduced the yield of product.

Structure Determinations. Diffraction-quality crystals were obtained by slow diffusion of petroleum ether into CH₂Cl₂ solutions at -30 °C. Experimental data for all determinations are presented in Table 3. X-ray intensity data were collected at 110(2) K on a Bruker-Nonius X8 APEX CCD area-detector diffractometer using Mo K α X-radiation. Several sets of narrow data "frames" were collected at different values of θ , for various initial values of ϕ and ω , using 0.5° increments of ϕ or ω . The data frames were integrated using SAINT;²⁴ the substantial redundancy in data allowed an empirical absorption correction (SADABS)²⁴ to be applied, on the basis of multiple measurements of equivalent reflections.

All structures were solved using conventional direct methods^{24,25} and refined by full-matrix least squares on all F^2 data using SHELXTL version 6.12,²⁵ with anisotropic thermal parameters assigned to all non-H atoms. The locations of the cage-carbon atoms were verified by examination of the appropriate internuclear distances and the magnitudes of their isotropic thermal displacement parameters. Cluster BH and CH hydrogen atoms, except those in **9**, were located in difference maps and allowed positional refinement; all other H atoms were set riding in calculated positions with

fixed isotropic thermal parameters defined as $U_{\text{iso}}(\text{H}) = 1.2[U_{\text{iso}}(\text{parent})]$.

Crystals of **10** contained a half-molecule of CH₂Cl₂ as solvate, along with each molecule of **10**, in the asymmetric fraction of the unit cell. The solvate lay close to an inversion center but was fully refined without difficulty. In crystals of **13** there was found an unidentified solvate, thought to be partial CH₂Cl₂, hexane, and/or pentane molecules. This was successfully modeled as four carbon atoms, for which anisotropic refinement was achieved; no attempt was made to include hydrogen atoms. For **9**, there was a large residual electron density peak ($\sim 3.7 \text{ e } \text{\AA}^{-3}$) close to the B(7)-Co(10) vector and closer to the former atom, possibly a result of some slight crystal twinning or disorder. This necessitated some constraint upon the thermal parameter of B(7) (EADP card in SHELXL), but solution and refinement were otherwise straightforward.

Acknowledgment. We thank the Robert A. Welch Foundation for support and the National Science Foundation Major Research Instrumentation Program (Grant No. CHE-0321214) for funds to purchase the Bruker-Nonius X8-APEX diffractometer.

Supporting Information Available: Full details of crystallographic analyses as a CIF file. This material is available free of charge via the Internet at <http://pubs.acs.org>.

OM060123D

(24) APEX 2, version 1.0; Bruker AXS, Madison, WI, 2003–2004.

(25) SHELXTL version 6.12; Bruker AXS, Madison, WI, 2001.